THE EVALUATION OF ELECTROOPTIC-SAMPLING INCLUDING DIFFRACTION AND APERTURE MASKING OF A TILTED ASTIGMATIC GAUSSIAN SAMPLING BEAM

W. Thomann, P. Russer

Institut für Hochfrequenztechnik, Technische Universität München, Arcisstr. 21, D-80290 München, Germany

ABSTRACT

Electrooptic-sampling necessitates a variety of probing geometries which include tilted astigmatic Gaussian sampling beams, whose field distribution has to be taken into consideration in the evaluation of the electrooptic-sampling signal. The generation of a tilted beam can be accomplished via an off-axis focussing lens. The formalism of ray matrices in geometrical optics is not adequate for waves with a field component in direction of the beam propagation. However, using Fresnels diffraction integral we derived the complex beam parameters for off-axis systems which are valid for half apex angles less than 12°. In addition, the sampling beam undergoes diffraction and aperture masking.

INTRODUCTION

The electrooptic-sampling method is a powerful measurement technique for noncontact [1] and noninvasive measurements of broadband hybrid and integrated planar microwave circuits. The method facilitates the measurement of time dependant signal waveforms at internal nodes [1] and the field distribution [2] of high frequency circuits. A versatile measurement setup facilitates the direct probing of circuits on electrooptic substrates and on arbitrary substrates by employing an external probe tip [1], [3]-[5]. The widespread applicability, however, requires the exact determination of the influence of the electric field components on the optical sampling beam and the resulting integral change of polarisation for a variety of probing geometries, beam parameters, different planar structures and substrate materials.

PROBING GEOMETRIES

Especially in the case of direct probing on electrooptic active substrates (i.e. GaAs, $LiNbO_3$, $LiTaO_3$), the planar structure itself imposes considerable constraints. The maximum electric field of a transmission line is located very close to its edges. Thus one is inclined to measure in this area in order to obtain a large signal-to-noise ratio. However, the spot size of the Gaussian sampling beam is limited and increases rapidly with distance to the focal position, as shown in Fig. 1. Thus, in order to evaluate the electric fields close to the conductor we need to take into consideration the diffraction and aperture masking imposed on the returning beam by the transmission line.

Focussing a beam perpendicular to the substrate on its backside results in the measurement of the potential on the substrate surface [5], however, also in a poor spatial resolution, limited by the beam radius ($w = 23\,\mu$m for $w_{\min} = 2\,\mu$m) on the substrate surface. On the other hand, focussing the beam on the substrate surface results in a high spatial resolution, however, also in diffraction and considerable blocking of the returning beam within $46\,\mu$m (Fig. 1) of the transmis-

TH 3F

0-7803-3246-6/96/$5.00 © IEEE

1996 IEEE MTT-S Digest

a: Offset lens

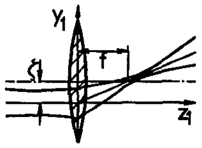

$$m_{12,y} = \cos\alpha \left[\left(1-\frac{s_1}{f}\right)^2+\left(\frac{z_{R1}}{f}\right)^2\right]^{-\frac{1}{2}}$$

$$w_{02,y} = m_{12,y}\, w_{01}$$

$$z_{R2,y} = m_{12,y}^2\, z_{R1}$$

$$s_{2,y} = f\cos^2\alpha + m_{12,y}^2\,(s_1 - f)$$

m: magnification w_0: beam radius s: position z_R: Rayleigh range, f focal distance; y: y-z beam, x-z beam transformed as in on-axis systems

b: Tilted beam

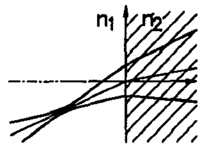

$$m_{12} = \frac{n_2}{n_1}$$

$$w_{02} = \frac{\cos\alpha_2}{\cos\alpha_1} w_{01}$$

$$z_{R2} = \frac{\cos^2\alpha_2}{\cos^2\alpha_1}\frac{n_2}{n_1} z_{R1}$$

$$s_{2d} = -\frac{\cos^2\alpha_2}{\cos^2\alpha_1}\frac{n_2}{n_1} s_{1h}$$

Tab. 1: Parameters of offset and tilted Gaussian beam.

sion line edge and interaction in the entire volume of the sampling beam. A probing geometrie which partially prevents these disadvantages is implemented with a tilted sampling beam. However, the convenient generation of a tilted Gaussian beam with a single off-axis focussing and collimating lens as well as the refraction on the substrate surface results in an astigmatic (ellipical) Gaussian beam. An astigmatic Gaussian beam exhibits a Gaussian distribution in two perpendicular planes through the beam axis, however, each minimum beam waist and beam waist position as well as diffraction angle are different. Table 1 shows the derived beam parameters.

CALCULATIONS

The beam profile of the Gaussian sampling beam, perturbed by an aperture can be calculated with Fresnels diffraction integral. Fig. 2 shows the field distribution of a Gaussian beam after diffraction on an aperture in the negative half-plane at the longitudinal position $z=0$. In the following examples we use a tilt angle of 1° and an ellipticity of 1% in order to simplify explanations. The integral is evaluated in transverse direction of the aperture, starting at the edge and integrating towards plus infinity, i.e. a sufficient distance.
We consider a Gaussian beam with the minimum beam radius at $z=0$ (Fig. 2, top) and the beam axis at the edge of the aperture $x = 0$. Thus, half of the beam is blocked by the aperture. In the near field we obtain considerable diffraction. However, normalization to the corresponding maximum of an unperturbed Gaussian beam, reveals a relaxation towards a Gaussian profile in the far field (i.e. two times the substrate thickness for round trip, $800\,\mu$m). This effect is limited to the symmetric case with a beam approaching an ideal Gaussian beam of half the amplitude and twice the width, corresponding to half of the incident power. The second blocking of the beam on its return path causes a reduction of the initial power to 25% .
Fig. 2 (bottom) depicts an unsymmetric case with a drastically varying field distribution. The position of the beam waist is located $400\,\mu$m past the aperture and already at the position $z=600\,\mu$m most of the optical power has shifted to the left half-plane, caused by the phase of the transmitted beam portion. The maxima approaches the position $x \approx -0.6\,w(z)$ and the shape scales with further increasing distance. Even though the direction of the beam is unperturbed, the intensity maxima travels with an angle of approx. $-1,7^\circ$. Diffraction patterns are considerable if the position of the beam axis to aperture edge is smaller than the beam radius, whereas 99% of the power is concentrated within 1.5 times the beam radius.

The evaluation of the electrooptic signal involves the field distribution of the planar structure itself, as well as the field distribution of the sampling beam with respect to amplitude and phase and its influence on the reflected intensity. The calculation of the influence of the electrical field on the optical field within the volume of interaction can be calculated with the volume-integral-method [5]. The calculation of the integral intensity of the reflected beam is performed by the absolute value of the squared integrand under consideration of the partially blocked return path.
The results are shown in Fig. 3 and yield: (i)

the symmetric case results in a 25% intensity of the reflected beam, excluding Fresnel reflections. Obvious is the rapid increase of intensity to about 50% up to a position of twice the beam radius and a gradual increase with distance; (ii) if focussed within the substrate we obtain an intensity of 10% at the aperture edge, however, the intensity increases rapidly and overrides the intensity of the symmetric case at a position of several beam radii; (iii) depending on the position of the sampling beam with respect to the transmission line edge, an optimization of the focus position may be performed; (iv) in the case of coinciding positions of aperture and beam waist the intensity may be represented by the product of two complementary error-functions (squares in Fig. 3). The results exclude the influence of an electric field and thus, the highest eo-sensitivity in the area of the beam waist and the transmission line edge.

MEASUREMENTS

The comparison of measurement and calculations of the intensity variation in the vicinity of the aperture edge is shown in Fig. 4. The measurement yields a minimal beam radius of $1.5\,\mu$m. With an optimization routine one can easily determine the beam parameters as well as the position of the transmission line edge. This in turn allows the correction of the electrooptic signal close to a transmission line edge and thus, a calibration of the measurement setup.

The measurement of the transverse field distribution of a $280\,\mu$m wide microstrip line on a $400\,\mu$m thick GaAs-substrat is shown in Fig. 5. The diagram depicts the electrooptic signal with rapidly decreasing amplitude for increasing transverse positions. Obvious is the characteristic decrease of the intensity caused by diffraction and aperture masking. Besides calculation, this effect can be measured as the dc-part of the processed lock-in-amplifier signal. Also shown is the calculated and fitted intensity dependence on the beam axis ($w_{\mathrm{min}} = 0,8\,\mu$m). The corrected electrooptic signal is depicted and shows the actual potential distribution close to the transmission line. Unfortunately, the dc-signal is not adequately filtered and digitized and, thus, introduces unnecessary errors in the corrected electrooptic signal.

CONCLUSION

The evaluation of electrooptic-sampling including diffraction and aperture masking of a tilted astigmatic Gaussian sampling beam has been demonstrated. The comparison of measurements and calculations shows a very good agreement.

REFERENCES

[1] T. Nagatsuma, T. Shibata, E. Sano, and A. Iwata, "Subpicosecond sampling using a noncontact electro-optic probe," *Appl. Phys. Lett.*, vol. 66, pp. 4001–4009, Nov. 1989.

[2] M. Mertin, A. Leyk, G. David, R.M. Bertenburg, S. Kosslowski, F. J. Tegude, I. Wolff, D. Jäger, and E. Kubalek, "Two-dimensional mapping of amplitude and phase of microwave fields inside a MMIC using the direct electro-optic sampling technique," in *IEEE MTT-S Digest*, (San Diego), pp. 1597–1599, 23rd-27th of May 1994.

[3] J. L. Freeman, S. R. Jeffries, G. A. Mourou, and J. A. Valdmanis, "Full field modelling of the longitudinal electrooptic probe," *Optics Letters*, vol. 12, pp. 765–766, 1987.

[4] M. Rottenkolber, W. Thomann, and P. Russer, "Characterization and optimization of electrooptic sampling by volume-integral-method and application of space-harmonic potential," in *IEEE MTT-S Digest*, (Atlanta, USA), 14th-18th of June 1993. pp. 265–268.

[5] W. Thomann, M. Rottenkolber, and P. Russer, "Optimization of electrooptic sampling by volume-integral method," *IEEE Trans. Microwave Theory Tech.*, vol. 41, pp. 2398–2399, Dec. 1993.

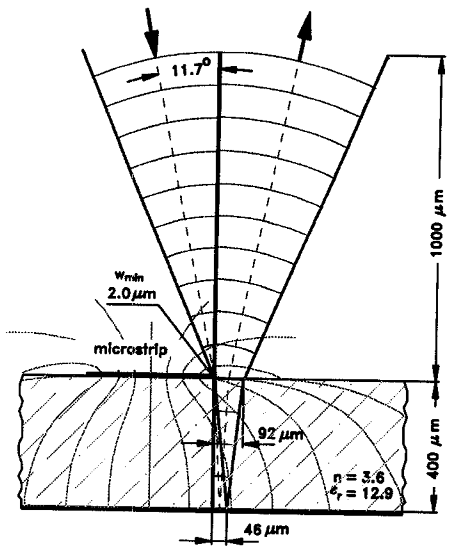

Fig. 1: Tilted Gaussian sampling beam.

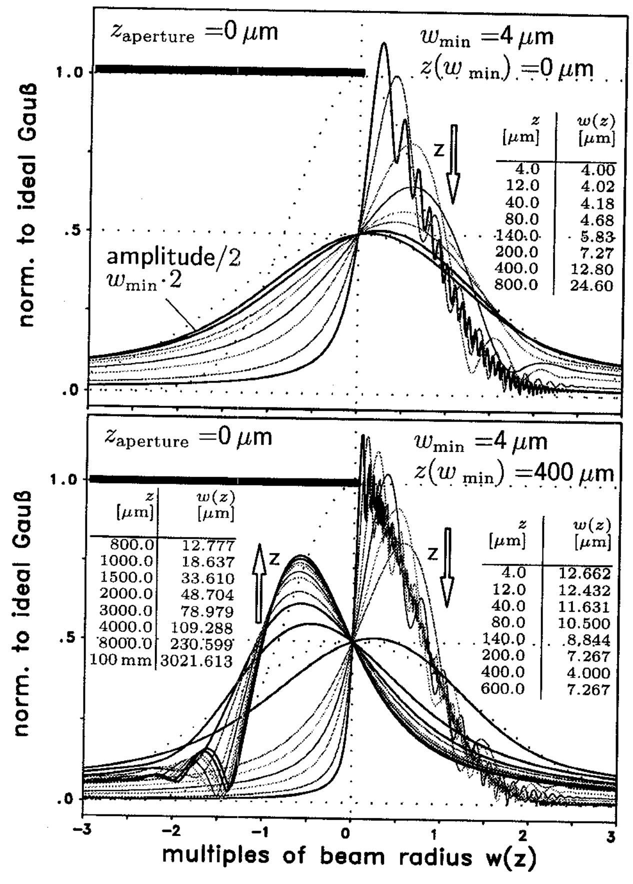

Fig. 2: Diffraction of Gaussian beam on aperture in the negative half-plane $-\infty < x < 0$ at the position $z = 0\,\mu$m; beam waist of $w_{min} = 4\,\mu$m at the position $z(w_{min}) = 0\,\mu$m (top) and $400\,\mu$m (bottom).

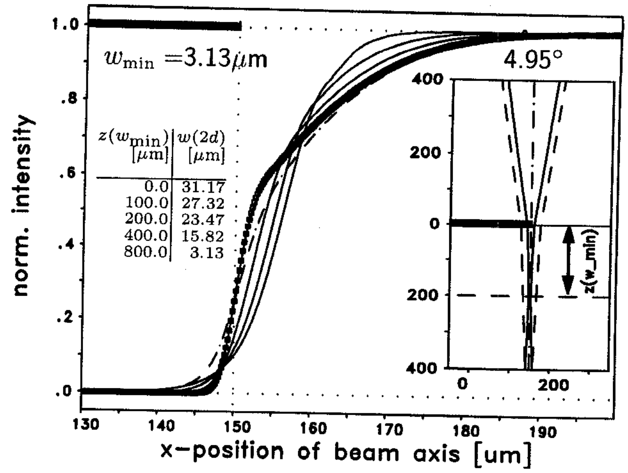

Fig. 3: Intensity of reflected sampling beam.

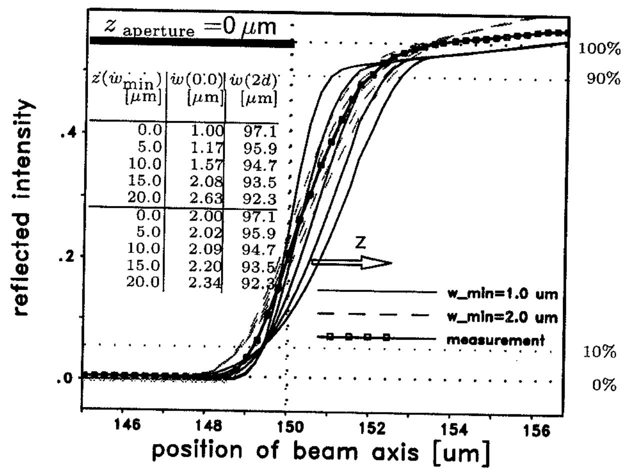

Fig. 4: Comparison of measurement and calculation of the intensity variation.

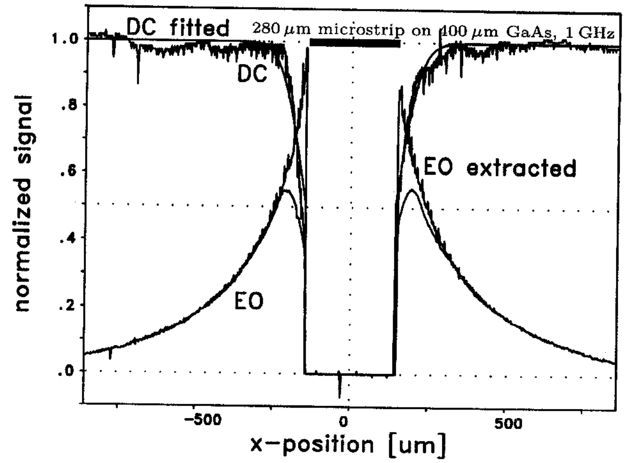

Fig. 5: EO-measurement ($1.3\,\mu$m semiconductor laser) of the field distribution across a $280\,\mu$m microstrip.